

## CoFe<sub>2</sub>O<sub>4</sub>/buffer layer ultrathin heterostructures on Si(001)

R. Bachelet,<sup>1</sup> P. de Coux,<sup>1,2</sup> B. Warot-Fonrose,<sup>2</sup> V. Skumryev,<sup>3</sup> J. Fontcuberta,<sup>1</sup> and F. Sánchez<sup>1,a)</sup>

<sup>1</sup>Institut de Ciència de Materials de Barcelona (ICMAB-CSIC), Campus UAB, 08193 Bellaterra, Spain

<sup>2</sup>CEMES-CNRS, 29 rue Jeanne Marvig, BP 94347, Toulouse Cedex 4, France

<sup>3</sup>Institució Catalana de Recerca i Estudis Avançats (ICREA), Barcelona, Spain, and Dep. de Física, UAB, 08193 Bellaterra, Spain

(Received 8 June 2011; accepted 7 September 2011; published online 19 October 2011)

Epitaxial films of ferromagnetic CoFe<sub>2</sub>O<sub>4</sub> (CFO) were grown by pulsed laser deposition on Si(001) buffered with ultrathin yttria-stabilized zirconia (YSZ) layers in a single process. Reflection high-energy electron diffraction was used to monitor in real time the crystallization of YSZ, allowing the fabrication of epitaxial YSZ buffers with thickness of about 2 nm. CFO films, with thicknesses in the 2–50 nm range were subsequently deposited. The magnetization of the CFO films is close to the bulk value. The ultrathin CFO/YSZ heterostructures have very flat morphology (0.1 nm roughness) and thin interfacial SiO<sub>x</sub> layer (about 2 nm thick) making them suitable for integration in tunnel (e.g., spin injection) devices. © 2011 American Institute of Physics. [doi:10.1063/1.3651386]

Device downsizing has been the causing factor of the continuous progress in microelectronics. But scaling is approaching a limit, and further improvements will finally require the integration of new materials.<sup>1</sup> Oxides with remarkable properties are good candidates. An example is the replacement of SiO<sub>x</sub> by high-k oxides such as HfO<sub>2</sub> in MOSFETs. Other complex oxides are also of high interest. However, in most of the targeted applications, they have to be crystalline and oriented (i.e., epitaxial) on silicon platforms, which is a challenging task regarding the dissimilarities between oxides and silicon, both structurally and chemically. Ferroelectric (FE) oxides are now starting to be used for FE random access memories as potential alternatives to flash memories.<sup>2</sup> In contrast to FE oxides and despite the expected bright future of spintronics in semiconductor technology,<sup>3–5</sup> the use of ferromagnetic (FM) oxides in microelectronic devices appears to be distant. This is probably due to the elusive integration of epitaxial FM oxides with silicon. Therefore, epitaxial growth on silicon wafers with controlled characteristics and properties comparable to those of films on oxide single-crystalline substrate is crucial in the development of new functional oxide-based heterostructures. A recent example is the successful preparation of the two-dimensional electron gas at interfaces between LaAlO<sub>3</sub> and SrTiO<sub>3</sub> (STO) on Si(001).<sup>6</sup> In this case, the STO film is a part of the functional heterostructure but can also act as a buffer layer. The use of a buffer layer is a common requisite for the integration of most of the complex oxides. STO can be grown by molecular beam epitaxy on Si(001) using well-established methods.<sup>7–10</sup> However, to integrate complex oxides with large lattice mismatch and/or chemical interaction with STO, different buffers have to be considered. In that case, yttria-stabilized zirconia (YSZ) is an alternative.<sup>11–15</sup> YSZ has been grown epitaxially on Si(001), with crystallization after reduction of the native oxide.<sup>16,17</sup> However, it had been found that in ultrathin YSZ films

islands are formed in the early growth stages, and although coalescence and flattening were observed for thicker YSZ films,<sup>16</sup> the roughness at the initial stage is a severe limitation that prevents the use of YSZ as a buffer for applications requiring an ultrathin buffer.

We have grown ultrathin (2 nm thick) YSZ films on Si(001) using reflection high-energy electron diffraction (RHEED) to monitor in real time the onset of YSZ epitaxy. Complementary to the RHEED characterization, ex-situ atomic force microscopy (AFM) was used to demonstrate that the ultrathin layers are extremely flat. We have integrated CoFe<sub>2</sub>O<sub>4</sub> (CFO) films with silicon, buffered with ultrathin YSZ, proving its suitability as a buffer layer. CFO and some other spinels such as NiFe<sub>2</sub>O<sub>4</sub> are FM and also electrical insulators at room temperature. Hence, they are suitable materials for devices such as spin filters,<sup>18,19</sup> and could be combined with FE to form artificial multiferroic systems.<sup>20,21</sup> These spinels have been grown epitaxially on Si(001), typically using CeO<sub>2</sub>/YSZ double buffer layers.<sup>20,22,23</sup> Here we report on the growth of CFO with a single YSZ buffer, with a total thickness of the CFO/YSZ heterostructures below 5 nm. The heterostructures are epitaxial, with very flat surface, sharp CFO/YSZ interface and thin interfacial SiO<sub>x</sub> layer. The ultrathin YSZ buffers can also be used to grow relatively thick FM CFO film (50 nm) with magnetization close to its bulk value and with high coercivity.

CFO/YSZ heterostructures were prepared by pulsed laser deposition in a single process on Si(001) substrates. A KrF excimer laser ( $\lambda=248$  nm) operating at 5 Hz was focused sequentially on ceramic targets at a fluence of  $\sim 1.2$  J/cm<sup>2</sup>. The Si(001) substrates were used without removing the native SiO<sub>x</sub>. A RHEED system working at 30 kV was used to monitor in real time the crystallization of YSZ after the SiO<sub>x</sub> reduction. Ultrathin YSZ buffers ( $\sim 2$  nm, after 100 laser pulses at  $\sim 0.02$  nm/pulse) were grown at 800 °C under base pressure ( $\sim 7 \times 10^{-7}$  mbar). Then, the substrate temperature was decreased to 500 °C or 550 °C and CFO films

<sup>a)</sup>Electronic mail: fsanchez@icmab.es.

were grown with different number of laser pulses to control the thickness (at  $\sim 0.007$  nm/pulse). Deposition started under base pressure and  $\sim 5 \times 10^{-4}$  mbar oxygen was introduced after 40 laser pulses. After 90 additional laser pulses the pressure was increased progressively until 0.1 mbar. The in situ RHEED characterization of the epitaxial relationships was complemented by x-ray diffraction (XRD). High resolution transmission electron microscopy (TEM) was conducted in cross-section geometry. AFM was used to investigate the surface morphology of the films. Magnetization loop was measured at 10 K by superconducting quantum interference device with magnetic field applied in the plane along Si[110].

The RHEED pattern of the Si(001) substrate in Fig. 1(a) was taken along the Si[100] direction at 800 °C. Bragg diffraction spots and Kikuchi lines are clearly observed in spite of the native  $\text{SiO}_x$ . Absence of  $2 \times 1$  reconstruction in the pattern along Si[110] (not shown here) confirmed the oxidation of Si(001). The pattern changed with YSZ deposition and a halo characteristic for an amorphous film was observed during the first 50 laser pulses, corresponding to a nominal YSZ

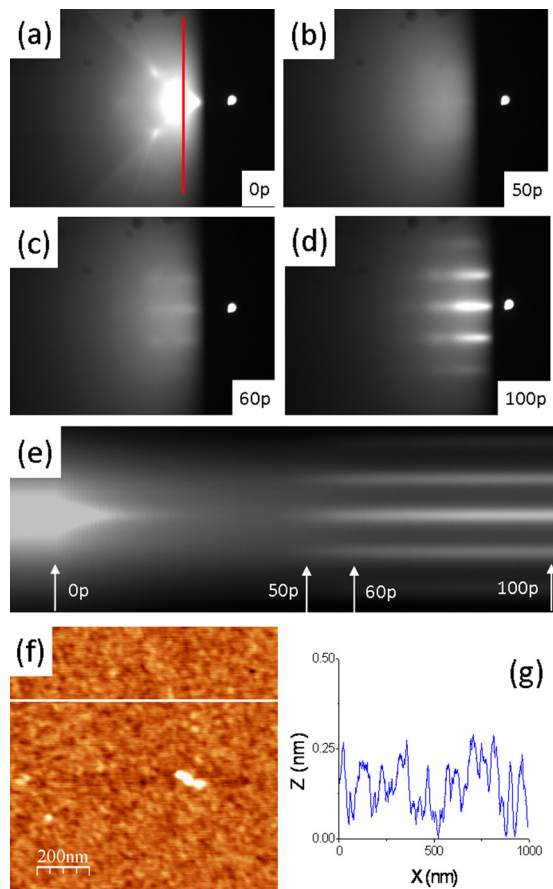


FIG. 1. (Color online) (a)–(d) RHEED patterns taken along Si[100] (a) of the Si(001) substrate and during deposition of YSZ, after (b) 50, (c) 60, and (d) 100 laser pulses. The respective grazing angles were  $1.6^\circ$  in (a), (b), and (c), and  $0.9^\circ$  in (d). (e) RHEED intensity profiles along the line in the Si[010] direction marked in (a) plotted as a function of deposition time. The grazing angle was  $1.6^\circ$ . Arrows in the bottom indicate the start of the deposition (0 laser pulses), 50 and 60 laser pulses, corresponding respectively to the patterns shown in panels (b) and (c) 100 laser pulses (end of the deposition). (f) AFM topographic image of the YSZ buffer, with (g) the corresponding height profile along the marked line in (f).

thickness of  $\sim 1$  nm [Fig. 1(b)]. With further increase of the thickness, diffraction spots become visible (see in Fig. 1(c) the pattern acquired after 60 laser pulses). The intensity of the Bragg spots increased with additional laser pulses defining the RHEED pattern characteristic of an epitaxial film (see Fig. 1(d)). It is concluded that a minimum amount of Y and Zr atoms has to be deposited on  $\text{SiO}_x$  to reduce it and then to form a crystalline YSZ epilayer on the bare Si(001) surface.<sup>16</sup> The time dependence of the RHEED line profiles plotted in Fig. 1(e) reflects these stages. Remarkably, the epilayer is flat (signaled by the streaky pattern). This observation was confirmed by AFM, revealing a low surface roughness of 0.1 nm (see Figs. 1(f) and 1(g)). Inhomogeneous YSZ crystallization on Si(001) had been earlier reported.<sup>16</sup> In contrast, the homogeneous crystallization reported here results in ultrathin YSZ films that are atomically flat and epitaxial from thickness of about 1.5 nm as detected by in situ RHEED.

CFO films were deposited on ultrathin YSZ buffer prepared as described above. The deposition started ( $\sim 40$  laser pulses, for  $\sim 0.2$  nm of CFO) in base pressure, and diffraction rings start to appear in the RHEED pattern signaling a polycrystalline growth. Introduction of relatively low pressure of oxygen ( $\sim 5 \times 10^{-4}$  mbar) oxidized the deposited CFO and enhanced the crystalline ordering. The diffraction patterns after 50 [Fig. 2(a)] and 100 laser pulses [Fig. 2(b)] quickly changed from rings to streaks that remain stable during the rest of the deposition. The streaky pattern at the end of the deposition [Fig. 2(c)] signals epitaxial growth and flat surface. Ex-situ AFM (see a topographic image and the

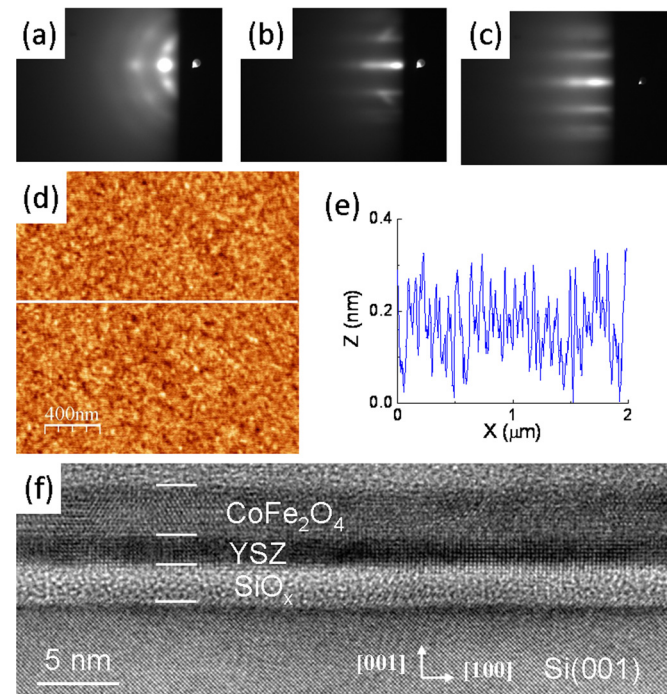


FIG. 2. (Color online) (a)–(c) RHEED patterns taken along Si[100] during growth of CFO at 500 °C acquired at a grazing angle of  $1.0^\circ$  after deposition of 50 (a) and 100 laser pulses (b). (c) Pattern taken at the end of the growth (400 laser pulses) at a grazing angle of  $1.6^\circ$ . (d) Topographic AFM image of the CFO film, with (e) the height profile along the marked line in (d). (f) Cross-section TEM showing the ultrathin epitaxial heterostructure.

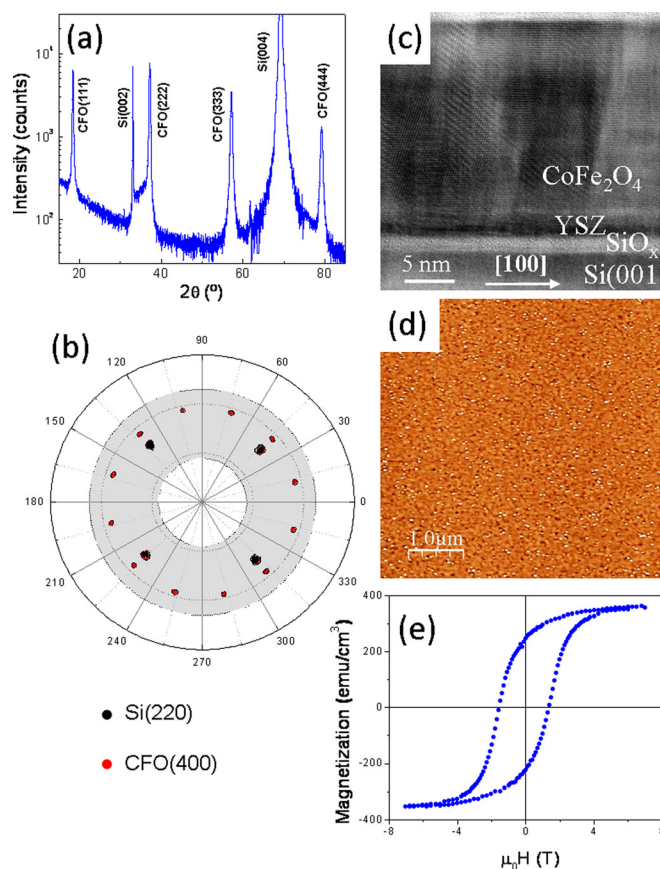


FIG. 3. (Color online) (a)–(b) XRD measurements of thick CFO grown at 550 °C on YSZ/Si(001):  $\theta$ - $2\theta$  scan (a) and pole figure of Si(220) and CFO(400) (b). (c) Cross-section TEM and (d) topographic AFM images. (e) Magnetization hysteresis loop measured at 10 K with the field applied in-plane along the Si[110] direction.

corresponding height profile in Figs. 2(d) and 2(e), respectively) confirms two-dimensional growth with very low roughness (rms = 0.1 nm). In Fig. 2(f) we show a cross-section TEM image of the ultrathin heterostructure. The high quality of the epitaxy of both CFO and YSZ layers (with respective thicknesses of 2.9 and 1.9 nm) can be appreciated. The narrow white band along the interface indicates the presence of an interfacial SiO<sub>x</sub> layer 2.4 nm thick. The SiO<sub>x</sub> layer in single YSZ buffer on Si(001) was thinner than 0.8 nm (a detailed microstructural study will be published elsewhere), and therefore it is concluded that the interfacial layer became slightly thicker during CFO growth due to oxygen diffusion through the YSZ buffer.

The stability of the buffer and YSZ/Si interface is crucial for applications requiring thicker functional layers. We have grown CFO films, around 50 nm thick, on ultrathin (~2 nm) YSZ buffers. The  $\theta$ - $2\theta$  XRD scan around symmetrical reflections only shows substrate and CFO(111) reflections [Fig. 3(a)]. The pole figure of Si(220) and CFO(400) reflections are given in Fig. 3(b). The twelve CFO(400) peaks, 30° apart in  $\varphi$ , signal the presence of four (111)-oriented crystal domains. Spinel (Ni,Zn)Fe<sub>2</sub>O<sub>4</sub> films were reported to form the same crystal variants on YSZ(001)

buffers,<sup>20</sup> and the same kind of epitaxy was found for CFO grown on double CeO<sub>2</sub>/YSZ(001) buffers.<sup>23</sup> The cross-section TEM image in Fig. 3(c) shows a SiO<sub>x</sub> interfacial layer around 2.8 nm thick (the YSZ layer is not distinguishable in the low resolution image). The surface is flat, with rms roughness of 0.3 nm [see Fig. 3(d)]. Finally, we present in Fig. 3(e) the magnetic hysteresis loop of this sample. The coercive field is ~1.5 T, and the saturation magnetization ~350 emu/cm<sup>3</sup>, close to the bulk value. Remarkably, the good magnetic properties and the surface flatness of CFO films grown on ultrathin YSZ buffers are very similar to those grown on thick buffer layers.<sup>23</sup>

In conclusion, flat and ultrathin YSZ epitaxial buffers can be grown on oxidized Si(001) using real time RHEED to monitor the onset of YSZ crystallization. This buffer permits the integration of epitaxial ferromagnetic spinel films, with thickness ranging from around 2 nm to tens of nm, presenting thin SiO<sub>x</sub> interfacial layer, very flat surface, and high magnetization.

Financial support by MICINN of the Spanish Government [Projects MAT2008-06761-C03, MAT2011-29269-C03, and CSD2007-00041] and Generalitat de Catalunya (2009 SGR 00376) is acknowledged.

<sup>1</sup>R. F. Service, *Science* **323**, 1000 (2009).

<sup>2</sup>Y. Fujisaki, *Jpn. J. Appl. Phys.* **49**, 100001 (2010).

<sup>3</sup>C. H. Li, O. M. J. van't Erve, and B. T. Jonker, *Nature Comm.* **2**, 245 (2011).

<sup>4</sup>D. R. McCamey, J. Van Tol, G. W. Morley *et al.*, *Science* **330**, 1652 (2010).

<sup>5</sup>R. Hanson and D. Awschalom, *Nature* **453**, 1043 (2008).

<sup>6</sup>J. W. Park, D. F. Bogorin, C. Cen *et al.*, *Nature Comm.* **1**, 94 (2010).

<sup>7</sup>R. A. McKee, F. J. Walker, and M. F. Chisholm, *Phys. Rev. Lett.* **81**, 3014 (1998).

<sup>8</sup>Y. Wei, X. Hu, Y. Liang *et al.*, *J. Vac. Sci. Technol. B* **20**, 1402 (2002).

<sup>9</sup>G. Niu, G. Saint-Girons, B. Vilquin *et al.*, *Appl. Phys. Lett.* **95**, 062902 (2009).

<sup>10</sup>J. M. Reiner, A. M. Kolpak, Y. Segal *et al.*, *Adv. Mater.* **22**, 2919 (2010).

<sup>11</sup>Z. Trajanovic, C. Kwon, M. C. Robson *et al.*, *Appl. Phys. Lett.* **69**, 1005 (1996); P. Perna, L. Mechin, M. P. Chauvat, P. Ruterana, C. Simon, and U. Scotti di Uccio, *J. Phys. Cond. Matter* **21**, 306005 (2009).

<sup>12</sup>J. Fontcuberta, M. Bibes, B. Martínez *et al.*, *J. Appl. Phys.* **85**, 4800 (1999); J. Fontcuberta, M. Bibes, B. Martínez *et al.*, *Appl. Phys. Lett.* **74**, 1743 (1999).

<sup>13</sup>C. Guerrero, J. Roldan, C. Ferrater *et al.*, *Sol. State Electr.* **45**, 1433 (2001).

<sup>14</sup>H. N. Lee, D. Hesse, N. Zakharov *et al.*, *Science* **296**, 2006 (2002).

<sup>15</sup>M. Dekkers, M. D. Nguyen, R. Steenwelle *et al.*, *Appl. Phys. Lett.* **95**, 012902 (2009).

<sup>16</sup>A. Bardal, T. Matthee, J. Wecker *et al.*, *J. Appl. Phys.* **75**, 2902 (1994).

<sup>17</sup>H. Ishigaki, T. Yamada, N. Wakiya *et al.*, *J. Ceram. Soc. Jpn* **109**, 766 (2001).

<sup>18</sup>U. Luders, A. Barthelemy, M. Bibes *et al.*, *Adv. Mater.* **18**, 1733 (2006).

<sup>19</sup>A. V. Ramos, M. J. Guittet, J. B. Moussy *et al.*, *Appl. Phys. Lett.* **91**, 122107 (2007).

<sup>20</sup>N. Wakiya, K. Shinozaki, and N. Mizutani, *Jpn. J. Appl. Phys.* **41**, 7242 (2002).

<sup>21</sup>N. Dix, R. Muralidharan, J. M. Rebled *et al.*, *ACS Nano* **4**, 4955 (2010).

<sup>22</sup>N. Wakiya, K. Shinozaki, and N. Mizutani, *Appl. Phys. Lett.* **85**, 1199 (2004).

<sup>23</sup>R. Bachelet, P. de Coux, B. Warot-Fonrose *et al.*, *Thin Solid Films* **519**, 5726 (2011).